ON COHERENT ELECTRON BREMSSTRAHLUNG

Yu. S. KOROBOCHKO, V. F. KOSMACH, and V. I. MINEEV

Leningrad Polytechnic Institute

Submitted to JETP editor December 25, 1964

J. Exptl. Theoret. Phys. (U.S.S.R.) 48, 1248-1256 (May, 1965)

Coherent bremsstrahlung is observed experimentally when low-energy (tens of keV) electrons traverse crystalline targets. It follows from the kinematics of the process that quasi-monochromatic bremsstrahlung beams could also be produced at primary electron energies of the order of several units or tens of MeV.

1. INTRODUCTION

THE coherent elastic interaction of electrons with the periodic potential of a lattice results in the well-known phenomenon of electron diffraction. A necessary condition for the observation of diffraction is small scattering of the electrons in a crystal sample; for this reason extremely thin films are used in experimental work.

An electron traversing a structure with a periodic potential, such as a single crystal, experiences periodic accelerations and decelerations; the electron then constitutes a moving and oscillating electric dipole.

The interaction with each harmonic of the potential induces emission at a definite frequency that varies with the angle of observation because of the Doppler effect. This emission is coherent in the sense that the electron radiates over many lattice spacings without loss of phase.

The energy of a coherent photon can be represented by $\epsilon_n = hvn/a$, where h is Planck's constant, v is the electron velocity, a is the lattice constant, and n is the index of the potential harmonic. For copper, with a = 3.61 A, $v/c = \beta = 0.5$, and n = 1, we obtain $\epsilon = 1.7$ keV. The threshold of coherent radiation depends on the condition that the photon energy cannot exceed the electron kinetic energy $E_k = mv^2/2 \geq hv/a$; therefore for copper $E_k = 46$ eV. The real detection threshold for lines will, of course, be higher because of multiple electron scattering.

Since both electron diffraction and coherent bremsstrahlung result from electron interaction with the harmonics of the lattice potential, the conditions for observing electron diffraction should also be sufficient conditions for observing coherent bremsstrahlung. With increasing crystal sample thickness accompanied by increasing disappearance of the diffraction pattern, coherent bremsstrahlung lines will be averaged out and only the ordinary continuous bremsstrahlung spectrum will remain.

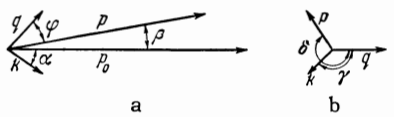

FIG. 1

2. KINEMATICS

We shall use the following notation: $\mathbf{p}_0$ and $\mathbf{p}$ are the electron momentum before and after the emission of a coherent quantum; $\mathbf{q}$ and $\mathbf{k}$ are the momentum acquired by the lattice and the photon momentum, respectively; α, β, and φ are the angles between the vector $\mathbf{p}_0$ and the vectors $\mathbf{k}$, $\mathbf{p}$, and $\mathbf{q}$ (Fig. 1); γ and δ are the angles between the projections of $\mathbf{k}$ and $\mathbf{p}$ and the projection of $\mathbf{p}_0$ on a plane perpendicular to itself (Fig. 1b).

Then, writing the conservation equations of energy (the energy transferred to the lattice being equated to zero because of the large mass of the latter) and of the three momentum components:

$$(\varepsilon_0^2 + p_0^2c^2)^{1/2} = (\varepsilon_0^2 + p^2c^2)^{1/2} + kc, \tag{1}$$

$$p_0 = q\cos\varphi + p\cos\beta + k\cos\alpha, \tag{2}$$

$$q\sin\varphi = p\sin\beta\cos\delta + k\sin\alpha\cos\gamma, \tag{3}$$

$$p\sin\beta\sin\delta + k\sin\alpha\sin\gamma = 0 \tag{4}$$

and eliminating p, β, and δ, we obtain the photon energy in the form

$$\varepsilon = c\frac{p_0q\cos\varphi - q^2/2}{p_0(1/\beta - \cos\alpha) + q(\cos\varphi\cos\alpha + \sin\varphi\sin\alpha\cos\gamma)} \tag{5}$$

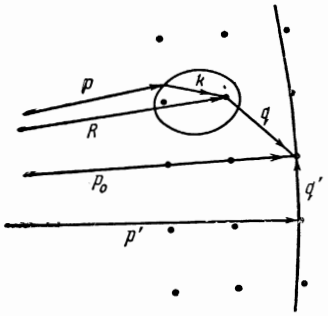

FIG. 2

A similar expression was used in [1] in analyzing certain questions concerning coherent bremsstrahlung from very high-energy electrons.

In (5) the structure with which the electron interacts depends on the set of possible values of q, φ, and γ. In the case of a single atom these quantities can assume values that vary continuously within certain limits, yielding the familiar bremsstrahlung spectrum.

For a single crystal q, φ, and γ are discrete; therefore ϵ also has corresponding discrete values. Equation (5) enables us to construct an extremely simple intuitive scheme of the process. Figure 2 represents the cross section of the reciprocal lattice (a primitive cubic lattice is assumed for simplicity) with the cell parameter $q_0 = h/a$.

A sphere of radius equal to the initial electron momentum p_0 is called the diffraction sphere or the Ewald sphere. It is easily seen that for points on this sphere the numerator of (5) vanishes; this corresponds to the absence of radiation. When any reciprocal lattice site coincides with the surface of the sphere, a beam of diffracted electrons appears in the corresponding direction; the resulting reflection spot in the electron diffraction pattern is represented by the vector $\mathbf{p}'$. At the same time the momentum $\mathbf{q}'$ is transferred to the lattice in a perpendicular direction. The momentum transfer represented by $\mathbf{q}$ corresponds to the emission of a coherent bremsstrahlung quantum.

The denominator of (5) can be rewritten as

$$\frac{p_0}{\beta} - p_0 \cos\alpha + q\cos(\widehat{\mathbf{qk}}) = \frac{p_0}{\beta}\left[1 - \frac{R\beta}{p_0}\cos(\widehat{\mathbf{Rk}})\right],$$

where $R\cos\widehat{Rk}$ is the projection of the vector difference $\mathbf{R} = \mathbf{p}_0 - \mathbf{q}$ on the direction of $\mathbf{k}$. Equation (5) thus becomes the equation of an ellipsoid in the polar coordinates

$$\varepsilon = \frac{A}{1 - B\cos(\widehat{\mathbf{Rk}})},\quad A = \frac{c\beta}{p_0}\left(p_0 q\cos\varphi - \frac{q^2}{2}\right),\quad B = \frac{R\beta}{p_0}.$$

The semimajor axis of the ellipsoid is always along $\mathbf{R}$, and its parameters depend on the primary electron energy as well as on the magnitude and direction of $\mathbf{q}$. The vector $\mathbf{q}$ starts at one focus of the ellipsoid; the starting point of $\mathbf{k}$ and the end-point of $\mathbf{p}$ lie on the ellipsoidal surface. For small primary electron energies, β and, accordingly, the ellipsoidal eccentricity B are close to zero; the ellipsoid thus becomes a sphere. The photon energy then does not depend on the direction of emission.

In the case $\beta \to 1$ the eccentricity B is close to unity (for relatively small values of q), and the ellipsoid becomes extremely elongated; this corresponds to a steep dependence of the photon energy on the emission angle. High-energy photons are emitted mainly in the R direction, i.e., practically in the direction of the primary electron momentum $\mathbf{p}_0$.

A similar diagram can obviously be constructed from (5) for each reciprocal lattice site lying inside the Ewald sphere. We thus obtain a complete kinematic picture of the interaction between electrons and all harmonics of the lattice potential. Because of thermal atomic motion the transfer of momentum will, of course, be discrete only for a relatively small number of reciprocal lattice sites lying close to the zeroth site (origin). However, since the probability of a transition decreases as q increases, [2] we can expect appreciable coherent effects in bremsstrahlung over a wide range of primary electron energies. As we know, when any reciprocal lattice site coincides with the surface of the Ewald sphere, a reflection spot is produced by elastically diffracted electrons at the corresponding point of the electron diffraction pattern. By measuring the angular distribution of electrons losing definite fractions of their energy through bremsstrahlung we should obtain a pattern of ellipsoidal cross sections arranged according to some law with respect to the elastic diffraction pattern, and defined by the intersections of the ellipsoids with a sphere of radius p that is concentric with the Ewald sphere. All points of this sphere obviously correspond to an identical value of p and therefore to an identical energy loss through bremsstrahlung. The pattern will correspond to the distribution of coherently and inelastically diffracted electrons. We shall now discuss some consequences of Eq. (5).

A. Photons are observed at the angle $\alpha = 0$. Then

$$\varepsilon = c\frac{q\cos\varphi - q^2/2p_0}{1/\beta - 1 + (q/p_0)\cos\varphi}$$

If $\mathbf{p}_0$ is now directed along one of the crystallo-

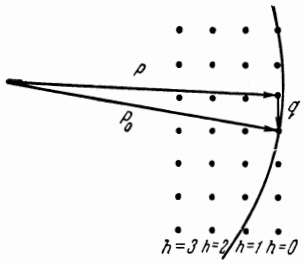

FIG. 3

graphic axes, q cos φ will be constant for all reciprocal lattice sites lying in some lattice plane perpendicular to p_0. The energies ϵ_h of the corresponding photons will be constant to within a term $q^2/2p_0$, which decreases as p_0 increases; in the case of fast electrons we have

$$\varepsilon_h = \frac{hcq_0}{\frac{1}{2}(E_0/E)^2 + hcq_0/E}$$

where h is the Miller index of the plane. For 50-MeV primary electrons in copper we obtain

$$\varepsilon_h = 3.5 \cdot 10^2 h / (5 + 7h) \text{ [MeV]}.$$

For h = 1 and 2 this gives 28.4 and 35.6 MeV, respectively.

B. Photons are observed at the angle $\alpha = \pi$, i.e., photons are registered in the direction opposite to that of the primary electrons. Then

$$\varepsilon = c\frac{q\cos\varphi - q^2/2p_0}{1/\beta + 1 - (q/p_0)\cos\varphi}. \quad (6)$$

For fast electrons $q^2/2p_0$ is small and $\epsilon = (\frac{1}{2})$ cq cos φ. With $q = q_0 h$ and $\varphi = 0$ in copper, $\epsilon_h = 1.7h$ [keV].

C. If in case B we select $\varphi = \pi/2 - \psi$ with $\psi \ll 1$, then $\epsilon = cq\psi/2$ and the photon energy can become very small. Thus ϵ will be in the region of visible light for copper with $q = q_0$ and 3.5×10^{-3} rad $> \psi > 1.8 \times 10^{-3}$ rad. If the primary electron energy is reduced so that $qcos\ \varphi \approx q\psi$ and $q^2/2p_0$ in the numerator of (6) are of comparable magnitudes, visible photons will be emitted at larger crystal inclination angles. For 50-keV electrons the range will be

$$0.91 \cdot 10^{-2} \text{ rad} < \psi < 1.08 \cdot 10^{-2} \text{ rad}.$$

The angle ψ is represented by the expression $\psi = 2\epsilon/cq_0 + q_0/2p_0$, corresponding to a transition to a site located in the immediate vicinity of the Ewald sphere surface (Fig. 3). Emitted photons accompanying transitions to different sites will vary greatly in energy, because the distance from a site to the surface of the sphere is a measure of the inelasticity of the process and varies greatly from site to site.

Radiative transitions from sites lying in the plane h = 0 (Fig. 3) are possible only if the sites lie inside the sphere. The number of these sites for small electron energies can be small because of the considerable curvature of the sphere (given by the term $q_0/2p_0$ in the last equation). Transitions to sites lying in planes of indices $h \geq 1$ will correspond to much harder (x-ray) photons. Radiation arising through a transition to each individual site will be completely polarized.

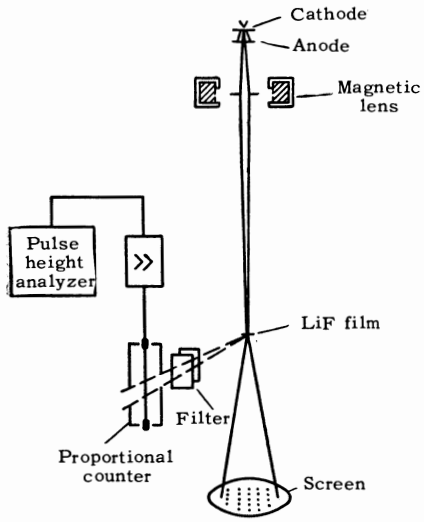

FIG. 4

D. The case of $\alpha \approx 0$ and $\psi \ll 1$ for very high-energy electrons has been studied in [3-5] and elsewhere. The bremsstrahlung now again exhibits well separated coherent peaks of polarized radiation resulting from transitions to individual reciprocal lattice sites.

3. EXPERIMENT

It was our aim to detect coherent bremsstrahlung from electrons in the usual 30—80-keV range of electron diffraction experiments. A thin (~ 500—1000 A) monocrystalline film of LiF was prepared by vapor deposition on the polished hot surface of a sodium chloride crystal which was subsequently dissolved in water. Lithium fluoride was chosen as the working substance because none of its characteristic lines are in the 1—5-keV region of the expected coherent peaks. The film was placed in an electron diffraction camera (Fig. 4) and was oriented with the aid of the diffraction patterns to produce an emerging electron beam that was as nearly perpendicular as possible to the [100] plane. The beam was focused on the film in order to prevent spectral averaging because of film wrinkling. The beam convergence angle at the film was $\sim 10^{-3}$ rad.

Since only a small number of coherent photons

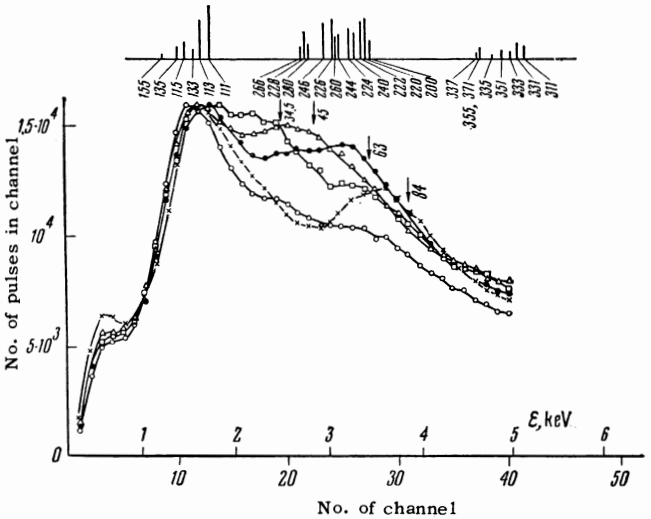

FIG. 5. Bremsstrahlung spectra for different primary electron energies: □ – 34.5 keV, △ – 45 keV, ● – 63 keV, × – 84 keV, ○ – 63 keV (for sharp slant of film). The curves for 34.5, 45, and 63 keV were measured on a single film. The registration time required for a single curve was ≈ 30 min.

were expected and since the wavelength of these photons depended on the angle of observation, it would have been difficult to use a diffraction grating for the spectral analysis. We therefore registered the spectra with a proportional counter that was filled with 90% Ar + 10% CH_4 at atmospheric pressure. Pulses from this counter were amplified and fed to a 100-channel pulse-height analyzer (AI-100). The detection angle was 67.5° with respect to the electron beam direction. The counter resolution was 17—19% as measured using the ~6-keV K line of Fe^{55}. The 1 × 10-mm counter window was covered with a 3—4-μ "lavsan" film. An electrostatic deflector placed before the counter prevented the entrance of electrons scattered by the LiF film; the number of these electrons exceeded the number of bremsstrahlung photons by a factor of 10^2—10^3. The counting rate of bremsstrahlung photons was ~100—300 pulses/sec. The stability of the entire registration system, as checked by means of the Fe^{55} calibration line, was not worse than 2—4% during an entire working day.

Some work was required to produce films free of impurities (mainly NaCl, some traces of which remained in the film when the rock salt crystals were dissolved in water). The impurity traces produced the characteristic lines of chlorine and other elements. The best of the prepared films gave clear electron diffraction patterns with a very small incoherent background. The thinness of the films obviated charging by the electron current traversing them.

Figure 5 shows the bremsstrahlung spectra measured for 34.5, 45, 63, and 84 keV. The steep rise of the curves in the region of the first twelve channels resulted from absorption of the soft spectrum in the counter window. The small bend in this region probably resulted from the 650-keV F1 line. The right-hand wing of each spectrum includes a broad maximum that we attribute to coherent bremsstrahlung. The principal properties of this maximum are:

1. It disappeared at a sharp slant of the film.
2. Its position varied with the primary electron energy.
3. The maximum became sharper, as a rule, as the quality of the electron diffraction pattern improved. When a spectrum was measured using a large primary electron current the quality of the electron diffraction pattern deteriorated during the exposure. Upon repeating the exposure we observed a much smaller relative peak size or even its complete disappearance.
4. Some spectra exhibited a very broad second peak of small amplitude.
5. When the film was oriented with the [110] plane perpendicular to the beam the maximum was shifted by a factor of about $\sqrt{2}$ in accordance with the changed interplanar spacing.

The properties 1 and 2 are illustrated in Fig. 5; the properties 4 and 5 are illustrated in Fig. 6. The top portion of Fig. 5 shows the photon energies corresponding to transitions to different reciprocal lattice sites for planes of indices h = 1,2, and 3. The energies were calculated from (5), written in the form

$$\varepsilon = \frac{cq_0 h}{1/\beta - \cos\alpha}\left[1 - \frac{\lambda}{2a}\,\frac{h^2+k^2+l^2}{h}\right] \times \left[1 + \frac{\lambda(h^2+k^2+l^2)^{1/2}}{a(1/\beta - \cos\alpha)} \times (\cos\alpha\cos\varphi + \sin\alpha\sin\varphi\cos\gamma)\right]^{-1} \qquad (6)$$

(where λ is the electron wavelength) for 63-keV primary electrons and for the reciprocal lattice sites closest to the zeroth site (origin). A real contribution to the coherent maximum can be expected only for the first four or five sites, because more distant sites are smeared out by the thermal motion of the lattice. The calculation assumed that the electron beam was strictly parallel to the appropriate crystallographic axis. A series of lines corresponds to the transitions to each plane. The highest energy appears for a transition with the smallest indices k and l for a given value of h. This transition is the series limit.

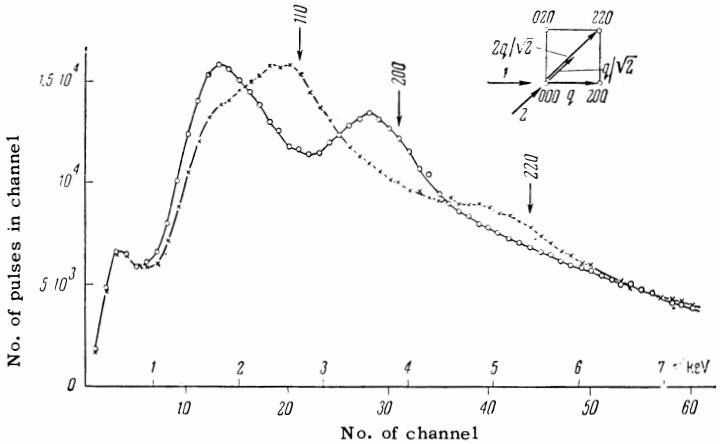

FIG. 6. Bremsstrahlung spectra for 84-keV electrons: o – electron beam perpendicular to the [100] plane, × – electron beam perpendicular to the [110] plane. Arrows 1 and 2 in the upper right-hand corner designate the electron beam directions relative to the lattice.

With increasing k and l the photon energy diminishes as the reciprocal lattice site approaches the Ewald sphere surface, where the energy vanishes.

The length of the vertical bar for each transition is proportional to its intensity, which was calculated following Heitler [2] with a correction for the atomic form factor. The inclusion of the latter has as its principal result that, in the case of LiF, transitions to sites having odd indices are about one-fourth as intense as those to sites having even indices.

Figure 5 shows the maximum corresponding to transitions to the h = 2 reciprocal lattice plane. The maximum for the h = 1 plane does not appear, evidently because of its relatively low intensity and because of its location in a spectral region that is inconvenient for observation. The maximum for the h = 3 plane should be relatively very weak. In addition, inaccurate orientation of the film, the mosaic structure etc. should reduce the degree of line grouping and therefore smear out the maximum to an increasing extent as h increases.

At all energies arrows indicate the expected locations of the series limits for transitions to the h = 2 plane. The agreement with the measurements appears to be satisfactory when it is considered that the majority of coherent photons in a series have energies below the series limit. We attribute the great width of the maximum to the spread of photon energies in the series and to the poor ($\sim 25-30\%$) counter resolution in the ~ 3-keV region.

Figure 6 shows the spectra measured on a single film having its [100] and [$\bar{1}$10] planes oriented perpendicular to an 84-keV electron beam. The curve for the [100] orientation resembles the corresponding curve in Fig. 5. On the curve for the [110] orientation the maximum is shifted to about 40% lower energy. We also observe on the right an additional low-amplitude smeared-out peak shifted to a 40—50% higher energy. Figure 6 also shows one plane of a reciprocal lattice cell marked with the directions of the electron beam and recoil momenta corresponding to the series limits. It is seen from Eq. (6) that the photon energies at the series limit are proportional to $q\cos\varphi$. Therefore, if for the [100] orientation these energies (for transitions to planes containing sites of even indices) are determined by the vectors q, 2q, 3q, ..., then for the [110] orientation the corresponding sequence is $q/\sqrt{2}$, $2q/\sqrt{2}$ etc. The positions of the series limits are indicated in Fig. 6 by arrows, which are seen to coincide satisfactorily with the locations of the maxima.

4. CONCLUSION

As already mentioned in paragraph A of Sec. 2, for primary electron energies of a few units or tens of MeV the bremsstrahlung spectrum can consist of well-separated narrow coherent peaks. The incoherent portion of the spectrum results from transitions to reciprocal lattice sites located far from the zeroth site. However, a calculation shows that the spectral density at the peak can be several tens of times greater than the spectral density of the incoherent spectrum in the region of this peak. In other words, it appears possible to obtain quasi-monochromatic γ-ray beams from electrons of relatively low energies, as is done in [4].

We also believe that the investigation of coherent bremsstrahlung, despite the complexity of the required procedure, can be of some interest for investigating the structure of solids, and especially of thin films. As we know, both the x-ray and electron diffraction methods "idealize" in-

vestigated structures in a certain manner. For example, if a sample possesses a mosaic structure, diffraction occurs only for microregions oriented at Bragg angles. The remaining regions do not participate in the formation of reflections and only strengthen the incoherent background. All microcrystals of a sample participate equally in the generation of bremsstrahlung. If diffraction gratings or other high-resolution means are used, the imperfections of a sample should broaden the line for each separate transition. The line width will thus be a measure of structural perfection.

In conclusion, we wish to thank M. A. Rumsh and A. P. Lukirskiĭ for their constant friendly assistance and numerous conferences, V. I. Perel' and O. V. Konstantinov for assistance in working out the theoretical aspects, and A. P. Komar for his continued interest. We also wish to thank P. V. Golubev for his rapid and excellent preparation of the mechanical portions of the apparatus, and N. N. Morozov for making the electron diffraction camera available.

[1] R. F. Mozley and J. de Wire, Nuovo cimento **27**, 1281 (1963).

[2] W. Heitler, The Quantum Theory of Radiation, 3rd Ed., Oxford U. Press, New York, 1954 (Russ. transl., IIL, 1956).

[3] H. Überall, Phys. Rev. **103**, 1055 (1956).

[4] Barbellini, Bologna, Diambrini, and Murtas, Phys. Rev. Letters 8, 454 (1962).

[5] M. L. Ter-Mikaélyan, JETP **25**, 296 (1953).

Translated by I. Emin
188